

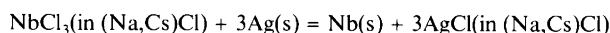
Chemistry of Niobium Chlorides in the CsCl–NaCl Eutectic Melt. 1. Electromotive Force Measurements of NbCl₃ in the CsCl–NaCl Eutectic Melt at Temperatures Between 600 and 700°C

Christian Rosenkilde and Terje Østvold*

Institute of Inorganic Chemistry, The Norwegian Institute of Technology, N-7034 Trondheim, Norway

Rosenkilde, C. and Østvold, T., 1994. Chemistry of Niobium Chlorides in the CsCl–NaCl Eutectic Melt. 1. Electromotive Force Measurements of NbCl₃ in the CsCl–NaCl Eutectic Melt at Temperatures Between 600 and 700°C. – Acta Chem. Scand. 48: 732–737 © Acta Chemica Scandinavica 1994.

EMF-data of NbCl₃ dissolved in the NaCl–CsCl eutectic melt have been obtained between 600 and 700°C using a niobium metal electrode and a mullite tube containing a silver wire dipping into an NaCl–CsCl eutectic melt containing 5 mol% AgCl as a reference electrode. At NbCl₃ concentrations below 0.2 mol%, the cell reaction:



was established in the galvanic cell. At higher concentrations, a black deposit containing sodium, caesium, chloride and niobium was precipitated on the electrode, and a new and unknown cell reaction was established. The calculated mean valence state of niobium in the precipitate was +3.5. In the dilute solutions of NbCl₃ studied, the entropy of mixing of liquid NbCl₃ in the NaCl–CsCl eutectic was ideal. The partial enthalpy of mixing of hypothetical liquid NbCl₃ in the eutectic was below –10 kJ mol⁻¹ for concentrations of NbCl₃ < 0.2 mol%. The hypothetical enthalpy and entropy of fusion for NbCl₃ have been calculated and $\Delta_{\text{fus}}S_{\text{NbCl}_3} = 52 \text{ J K}^{-1} \text{ mol}^{-1}$ and $\Delta_{\text{fus}}H_{\text{NbCl}_3} \geq 47 \text{ kJ mol}^{-1}$.

Electrolysis from molten salts is an interesting route to obtain pure niobium metal, and during the last three decades there have been several investigations on the electrochemistry of niobium in molten salts. Mellors and Senderof¹ showed that niobium can be electrodeposited from alkali fluoride melts. From an economical and environmental point of view, however, reduction of niobium from alkali chloride melts may be more attractive. In spite of many investigations on the electroreduction of niobium from liquid alkali chlorides, the reduction mechanism is still a matter of discussion. Polyakov *et al.*² claim that the reduction takes place in two steps, $\text{Nb}^{5+} + \text{e}^- = \text{Nb}^{4+}$ and $\text{Nb}^{4+} + 4\text{e}^- = \text{Nb}$, while Picard and Bocage³ and Lantelme *et al.*⁴ report a three-step reduction: $\text{Nb}^{5+} + \text{e}^- = \text{Nb}^{4+}$, $\text{Nb}^{4+} + \text{e}^- = \text{Nb}^{3+}$ and $\text{Nb}^{3+} + 3\text{e}^- = \text{Nb}$. Although there is dissention concerning the number of electrons transferred in the last step, Kuznetsov *et al.*⁵ and others^{2–4} agree that the reduction step to the metal is not of the simple reversible kind. Polyakov *et al.*² involve a dimerisation reaction. On the other hand, Lantelme *et al.*⁴ and Kuznetsov *et al.*⁵ claim

that a precipitation of an insoluble, lower-valent niobium compound takes place on the electrode and makes the reduction process more complex.

Since there are disagreements concerning the reduction of niobium in molten salts, and since most investigations employ transient electrochemical methods, it appears appropriate to study the system by other methods. It is the aim of this work to investigate the equilibrium between metallic niobium and dissolved niobium chlorides, in particular the influence of temperature and concentration of the niobium chlorides on the equilibrium electrode reaction using EMF measurements.

While NbCl₅ has a large solubility in alkali chloride melts,⁶ the solubility of NbCl₃ is reported to be low. Dartnell *et al.*⁷ report a 0.071 mol% solubility of NbCl₃ in a LiCl–KCl eutectic melt at 531°C. Lantelme *et al.*⁴ report, in their voltametric studies of niobium chlorides in the LiCl–KCl eutectic melt below 630°C, that a non-metallic precipitate was formed on the cathode during reduction. Above 630°C a coherent niobium deposit was formed. Kuznetsov *et al.*⁵ report similar results. Ivanovskii and Krasil'nikov⁸ and Nakagava and Hirabayashi¹⁰ report that NbCl₂ is stable in the melt, while

* To whom correspondence should be addressed.

Saeki *et al.*⁹ claim that NbCl_{2.67} is the dissolved niobium chloride in equilibrium with niobium metal in the LiCl–KCl eutectic melt. Vasin *et al.*,¹¹ however, found that NbCl₂ undergoes disproportionation according to the reaction $2\text{NbCl}_2 = \text{Nb} + \text{NbCl}_3$ when introduced to an alkali chloride melt. Picard and Bocage³ performed EMF measurements of Nb/Nb(III) in the LiCl–KCl eutectic melt at 450°C. They found that the standard potential versus the standard chlorine electrode using 1 molal NbCl₃ as standard state was $E_{\text{Nb}/\text{Nb(III)}}^\circ = -1.44$ V. Lantelme *et al.*⁴ used voltametry, obtaining $E_{\text{Nb}/\text{Nb(III)}}^\circ = -1.48$ V. Yang *et al.*¹² used EMF to measure the equilibrium between niobium chlorides and niobium metal in the LiCl–KCl eutectic melt. They found that at low concentrations of niobium-chlorides, Nb(III) was the equilibrium valence state, while at higher concentrations, higher-valent niobium chlorides coexisted with Nb(III). In a similar study in the same eutectic melt, Suzuki¹³ concluded that NbCl_{2.67} was the niobium chloride in equilibrium with Nb metal. We have chosen to work in the CsCl–NaCl eutectic melt primarily because this eutectic has a low melting point. The eutectic LiCl–KCl has a lower melting point, but LiCl is more difficult to dehydrate. Moreover, we have used the same eutectic in other parts of our study on the chemistry of niobium chloride melts.^{14,15}

Experimental

Equipment and chemicals. The chemicals used and purification procedures are given in Table 1. Since niobium chlorides have a very high affinity for O²⁻ ions in melts, a base melt practically free from oxides was needed for our investigations. A sample of the pure CsCl–NaCl eutectic melts was taken from the crucible at 650°C. The sample was analysed for oxide impurities by dissolving it in 50 ml distilled and ion-exchanged water while monitoring the pH. Before addition of the sample, the pH was 5.32. After addition of 1.3537 g of the eutectic, the pH increased to 5.37. This change in pH corresponds to a basic oxide content in the eutectic of 1.4×10^{-8} mol%. The pH after addition of 0.2 mg Na₂CO₃ to the solution was 8.9, indicating no buffer capacity. The synthesized NbCl₃ was analysed by precipitating in HNO₃. The precipitate was filtered, and the filtrate was ignited at 900°C

Table 1. Producers and purification procedures of the chemicals used.

Chemical	Producer and purification
CsCl	Fluka > 99.9%, dried with HCl and recrystallised
NaCl	Merck p.a., recrystallised
NbCl ₃	Made from sublimed NbCl ₅ (Alfa grade 1) and Nb (Alfa > 99.9%) according to Schäfer and Dohman ¹⁶
Nb	Alfa > 99.9%
AgCl	Fluka > 99% dried under vacuum at 150°C

and weighed. The Nb₂O₅ thus obtained gave an average valence state of Nb of 3.00–3.05. All experiments and handling of salts were carried out in an argon-filled glove box with water content <1 ppm and oxygen amount <5 ppm. A schematic diagram of the electrochemical cell mounted in the furnace is shown in Fig. 1. The reference electrode was a mullite tube closed in one end ($\phi = 10 \times 6$ mm Morgan Impervious Mullite, UK) with a silver wire dipping into a NaCl–CsCl eutectic melt containing 5 mol% AgCl. The indicator electrode was a niobium rod (5×50 mm) screwed onto a nickel rod ($\phi = 2.5$ mm). The temperature in the melt was measured with a calibrated thermocouple (Pt/Pt, 10% Rh). The thermocouple was immersed into the melt in such a way that only the wires were in contact with the melt, and a platinum crucible was used as container. The furnace used was a Kanthal-wound vertical and tubular furnace controlled with a Eurotherm controller. The furnace was mounted under the glove box in such a way that the experimental cell could be handled from the inside of the box. The temperature in the melt was stable within $\pm 2^\circ\text{C}$ during a constant-temperature measurement. Inductive

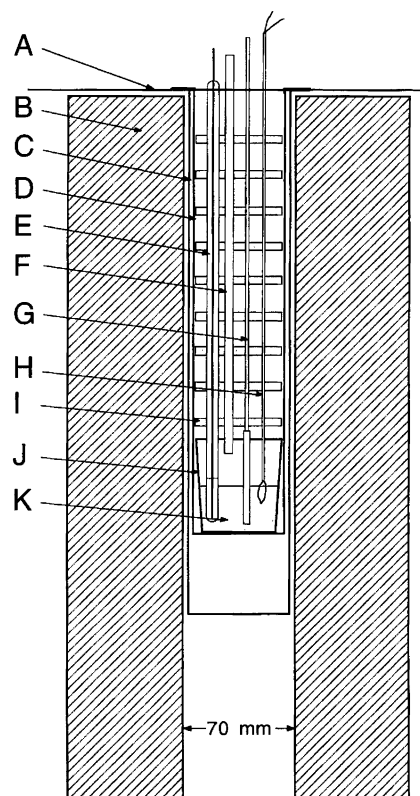


Fig. 1. Schematic diagram of the cell. (A) Bottom of glove box, (B) furnace, (C) stainless steel well with gas tight connection to glove box, (D) silica cell, (E) reference electrode (Mullite tube with a NaCl–CsCl eutectic melt containing 5 mol% AgCl and a silver wire dipping into the melt), (F) silica addition tube, (G) nickel rod connected to a niobium electrode, (H) two-bore Alsint rod for thermocouple, (I) Alsint radiation shields, (J) platinum crucible, (K) NaCl–CsCl eutectic melt with NbCl₃.

influences from the furnace on the electrochemical cell were avoided by a stainless-steel tube positioned between the inside walls of the furnace and the quartz cell (Fig. 1).

Experimental procedure. A silica cell containing the Pt crucible, radiation shields of Alsint, the thermocouple, a silica addition tube and the reference electrode, was introduced into the furnace. The temperature was raised to 700°C and kept at that temperature for 24 h to remove adsorbed water from the cell. Then 6.30 g NaCl and 33.70 g CsCl were added. When the salts had melted, the temperature was lowered to 600°C. The Nb electrode was introduced, and the voltmeter (a Keithley 617 electrometer) was connected to the electrodes. An *x-t*-recorder was used to monitor the EMF. Before the first addition of NbCl₃, the EMF was unstable. The first addition of NbCl₃ (15.9 mg) took place 24 h after addition of the alkali chlorides. The temperature was raised in steps of 25°C up to 700°C, and the EMF was recorded at each temperature step when the EMF was stable within ±1 mV. To check the stability of the reference electrode and the composition of the melt, the temperature was reduced to one of the lower temperatures and the EMF was again recorded. The temperature was then reduced to 600°C and more NbCl₃ added to the melt. This procedure was repeated for several compositions of NbCl₃.

Correction for thermoelectric potentials. There was a large temperature difference between the melt and the top of the cell, where the wires from the electrodes to the potentiometer were connected. Since the materials were different in the two electrodes, there was a thermoelectric potential included in the measured potential that must be corrected for. This potential was measured as a function of temperature by connecting a silver wire to the Nb tip of the electrode in a separate experiment, and can be described by the relation $E_{\text{thermo}}/\text{mV} = -4.94 + 0.0312T/^\circ\text{C}$ ($550 < T/^\circ\text{C} < 750$). The silver wire is the positive pole.

Principles

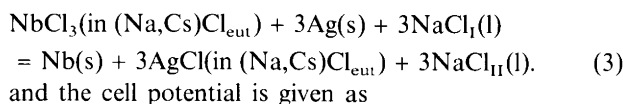
The electrode reactions for the cell studied:

Ag | 5 mol% AgCl in (Na,Cs)Cl_{eut} || Mullite | NbCl₃ in (Na,Cs)Cl_{eut} | Nb
can be written as



if the Nb/Nb(III) couple is the current-determining redox pair at the Nb electrode. Since Mullite is an Na⁺ conductor,¹⁷ there is a transport of Na⁺ through the mullite tube. This gives a net transfer of NaCl from the left (I) to the right-hand (II) side of the cell. The total cell

reaction may under the above assumption be written as:



$$E = E^\circ + \frac{RT}{3F} \ln \frac{a_{\text{NbCl}_3} a_{\text{Ag}}^3 a_{\text{NaCl(II)}}^3}{a_{\text{AgCl}}^3 a_{\text{Nb}} a_{\text{NaCl(I)}}^3} \quad (4)$$

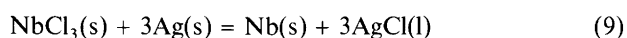
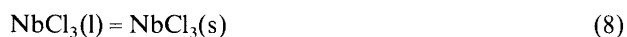
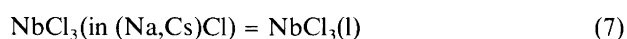
Using pure-component standard states [Nb(s), Ag(s), AgCl(l) and NbCl₃(l)], we obtain $a_{\text{Nb}} = a_{\text{Ag}} = 1$. Since both x_{AgCl} and x_{NbCl_3} are below 0.05, $a_{\text{NaCl(I)}} \approx a_{\text{NaCl(II)}}$ and

$$E = E^\circ - \frac{RT}{F} \ln a_{\text{AgCl}} + \frac{RT}{3F} \ln a_{\text{NbCl}_3} \quad (5)$$

Since Cl⁻ is the major anionic species in this melt, $x_{\text{Cl}} \approx 1$, and eqn. (5) takes the form

$$E = E^\circ - \frac{RT}{F} \ln x_{\text{AgCl}} \gamma_{\text{AgCl}} + \frac{RT}{3F} \ln x_{\text{NbCl}_3} \gamma_{\text{NbCl}_3} \quad (6)$$

Assuming that Henry's law is valid for NbCl₃ in the dilute range ($x < 0.01$), a plot of E versus $\log x_{\text{NbCl}_3}$ at constant temperature should yield a straight line with slope $R \ln 10 T / 3F$ if our assumption concerning the redox couple at the Nb electrode is correct. By varying the temperature at each composition, thermodynamic data for the cell reaction may be found. Thermodynamic data for pure liquid NbCl₃ are not given, and such data are needed to determine E° . However, we can obtain data on the sum of the enthalpy of fusion and the partial enthalpy of mixing of the hypothetical NbCl₃ by the procedure given below. Neglecting the small difference in the properties of NaCl in the two half-cells, the overall cell reaction, eqn. (3), is the sum of the following four reactions:



The enthalpy and entropy change for the cell reaction are thus the sum of the individual enthalpy and entropy changes for these four reactions. From the first reaction the partial enthalpy and entropy of mixing of the hypothetical pure liquid NbCl₃ in the (Na,Cs)Cl melt may be obtained. The second gives the freezing reaction of hypothetical pure liquid NbCl₃. The third reaction is the standard cell reaction if pure solid NbCl₃ is used as standard state. The thermodynamic data for this reaction may be found in the literature. The enthalpy and the entropy for the last reaction can also be found in the literature. Thus the enthalpy and entropy for eqn. (3) may be given as

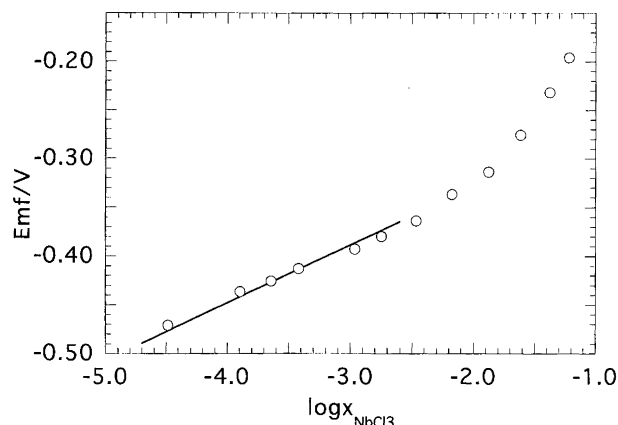


Fig. 2. EMF plotted versus $\log x_{\text{NbCl}_3}$ at 848 K and $x_{\text{AgCl}} = 0.05$. \circ Experimental data. (—) Calculated for $n=3$.

$$\Delta H[\text{eqn.}(3)] = -\Delta \bar{H}_{\text{NbCl}_3} - \Delta_{\text{fus}} H_{\text{NbCl}_3} + \Delta H^\circ[\text{eqn.}(9)] + 3\Delta \bar{H}_{\text{AgCl}} \quad (11)$$

$$\Delta S[\text{eqn.}(3)] = -\Delta \bar{S}_{\text{NbCl}_3} - \Delta_{\text{fus}} S_{\text{NbCl}_3} + \Delta S^\circ[\text{eqn.}(9)] + 3\Delta \bar{S}_{\text{AgCl}} \quad (12)$$

Results

In Figs. 2 and 3 the EMF is plotted versus $\log x_{\text{NbCl}_3}$ for two separate experiments, and a change in the slope at

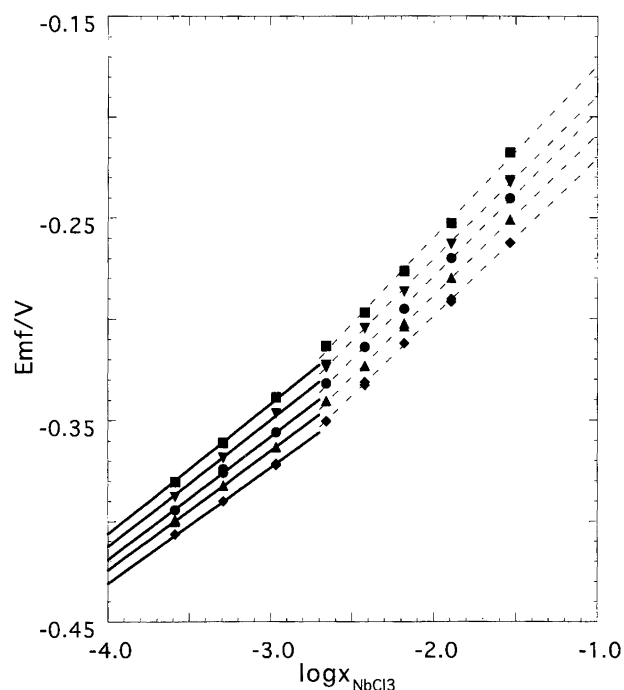


Fig. 3. EMF plotted versus $\log x_{\text{NbCl}_3}$ at five temperatures, T/K : \blacklozenge , 873; \blacktriangle , 898; \bullet , 923; \blacktriangledown , 948 and \blacksquare , 973. $x_{\text{AgCl}} = 0.05$. (—) Calculated for $n=3$. (---) Linear regression lines.

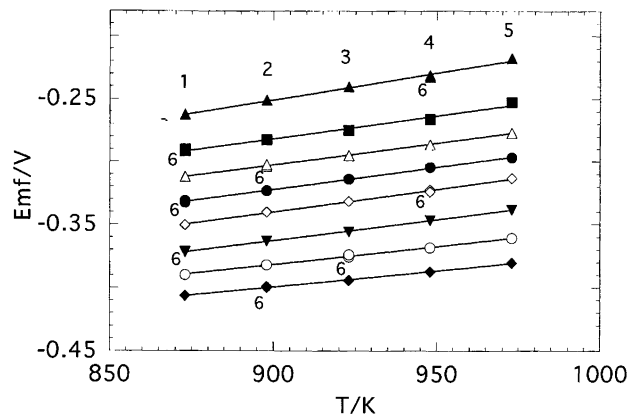


Fig. 4. EMF plotted versus temperature at eight different NbCl_3 concentrations, $x_{\text{AgCl}} = 0.05$. The equilibrium potentials were measured in the sequence: 1, 2, 3, 4, 5, 6. $\log x_{\text{NbCl}_3} = \blacklozenge$, -3.59 ; \circ , -3.29 ; \blacktriangledown , -2.96 ; \diamond , -2.66 ; \bullet , -2.42 ; \triangle , -2.18 ; \blacksquare , -1.89 and \blacktriangle , -1.54 . (—) Linear regression lines.

$\log x_{\text{NbCl}_3} \approx -2.7$ (0.2 mol% NbCl_3) is observed. At this composition, a black deposit was formed on the Nb electrode. The time needed to reach stable potentials (± 1 mV) after a change in the temperature increased with increasing concentrations of NbCl_3 . At low concentrations (< 0.2 mol% NbCl_3), 8–12 h were needed, while at high concentrations, as much as 24 h was necessary. This indicates that the cell reaction changes at NbCl_3 concentrations higher than 0.2 mol%. In Fig. 4 the EMF is plotted versus temperature for different values of $\log x_{\text{NbCl}_3}$.

Discussion

Cell reaction. In Table 2 the number of electrons, n , transferred in the cell reaction is calculated from the slope of EMF vs. $\log x_{\text{NbCl}_3}$ when $\log x_{\text{NbCl}_3}$ is < -2.7 . Values close to 3 are obtained, and the full lines drawn in Figs. 2 and 3 show calculated potentials for $n=3$. A reasonable agreement between calculated potentials and experimental data is observed. Since there is a change in $\partial E/\partial \log x_{\text{NbCl}_3}$ around $\log x_{\text{NbCl}_3} \approx -2.7$ (Figs. 2 and 3), and since a precipitate was observed on the Nb electrode at this and higher NbCl_3 concentrations, a new cell

Table 2. Values of n in the Nernst equation at six different temperatures calculated from $\partial E/\partial \log x_{\text{NbCl}_3}$ for $\log x_{\text{NbCl}_3} < -2.7$.

$T/^\circ\text{C}$	$\partial E/\partial \log x_{\text{NbCl}_3}/\text{V}$	n
575	0.0534	2.86
600	0.0554	3.10
625	0.0589	3.04
650	0.0620	2.96
675	0.0655	2.87
700	0.0673	2.87

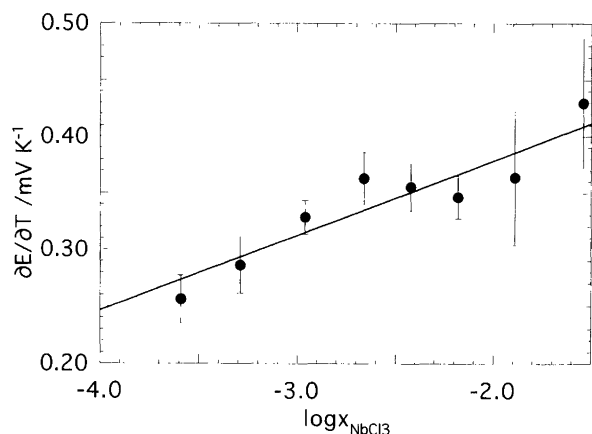


Fig. 5. $\partial E/\partial T$ plotted versus $\log x_{\text{NbCl}_3}$. Error bars are based on a 95% confidence interval for $\partial E/\partial T$. (—) Line with slope $\partial^2 E/(\partial T \partial \log x_{\text{NbCl}_3})/\text{mV K}^{-1} = 10^3 R \ln 10/3F$ obtained by assuming ideal entropy of mixing of NbCl_3 .

reaction probably occurs at $\log x_{\text{NbCl}_3} \approx -2.7$. Above this concentration the potential continues to increase with increasing NbCl_3 concentrations. The cell reaction must therefore still depend on the dissolved NbCl_3 , and the EMF of the cell may be established by a reaction between the dissolved NbCl_3 and a precipitated niobium-containing salt.

Calculation of thermodynamic data. If the entropy of mixing of dilute solutions of NbCl_3 is ideal, $\Delta \bar{S}_{\text{NbCl}_3} = -R \ln x_{\text{NbCl}_3}$, and the plot of $\partial E/\partial T$ versus $\log x_{\text{NbCl}_3}$ (Fig. 5) should give a straight line at low concentrations of NbCl_3 , since $\partial^2 E/(\partial T \partial \ln x_{\text{NbCl}_3}) = R/3F$. The full line in Fig. 5 represents this ideal slope. Error bars give the uncertainties in $\partial E/\partial T$. In view of the low concentrations and the present data, ideal entropy of mixing of NbCl_3 can be assumed below 0.2 mol% NbCl_3 . Above this weight in concentration of NbCl_3 , the concentration of NbCl_3 in the melt is unknown, owing to the precipitate formed on the electrode.

Equations (11) and (12) can be used in the relation $\Delta G = -nFE$ to relate the measured potential to thermodynamic data of the cell reaction. Since our melts are dilute in NbCl_3 and AgCl , we obtain

$$-3FE = -\Delta \bar{H}_{\text{NbCl}_3} - \Delta_{\text{fus}} H_{\text{NbCl}_3} + \Delta_r H^\circ [\text{eqn. (9)}] + 3\Delta \bar{H}_{\text{AgCl}} - T\{R \ln x_{\text{NbCl}_3} - \Delta_{\text{fus}} S_{\text{NbCl}_3} + \Delta_r S^\circ [\text{eqn. (9)}] - 3R \ln x_{\text{AgCl}}\} \quad (13)$$

Rearranging this expression, we get

$$RT \ln x_{\text{NbCl}_3} - 3FE = \{-\Delta_{\text{fus}} H_{\text{NbCl}_3} + \Delta_r H^\circ [\text{eqn. (9)}] - \Delta \bar{H}_{\text{NbCl}_3} + 3\Delta \bar{H}_{\text{AgCl}}\} - T\{-\Delta_{\text{fus}} S_{\text{NbCl}_3} + \Delta_r S^\circ [\text{eqn. (9)}] - 3R \ln x_{\text{AgCl}}\} = A - TB \quad (14)$$

By plotting the left-hand side of eqn. (14) versus temperature, a straight line should be obtained, and A and B

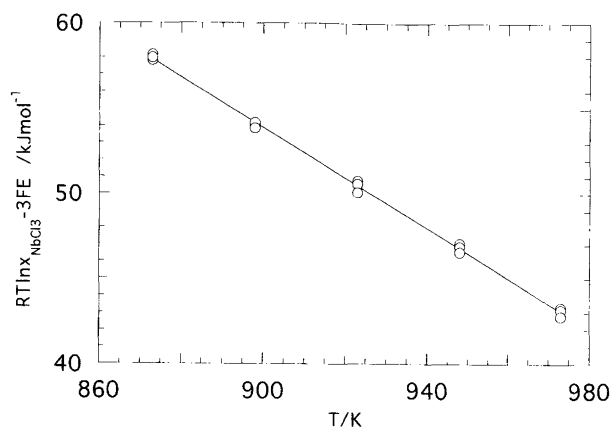


Fig. 6. $RT \ln x_{\text{NbCl}_3} - 3FE$ plotted versus the temperature for $x_{\text{AgCl}} = 0.05$ and $x_{\text{NbCl}_3} < 0.002$. (—) Linear regression line giving $RT \ln x_{\text{NbCl}_3} - 3FE/V = 187 \times 10^3 - 148 T/K$.

can be determined. From the regression line given in Fig. 6 where only EMF data for $\log x_{\text{NbCl}_3} < -2.7$ have been used, the slope, $B = 148 \pm 3 \text{ J K}^{-1} \text{ mol}^{-1}$ using a 95% confidence interval for the slope. On the basis of the slope, B , and the uncertainty in B , the intercept of 0 K, $A = 187 \pm 3 \text{ kJ mol}^{-1}$, is obtained. The partial entropy and enthalpy of mixing of AgCl in the $\text{NaCl}-\text{CsCl}_{\text{eutectic}}$ can be estimated from the enthalpy and entropy of mixing in the binaries $\text{AgCl}-\text{NaCl}$, $\text{AgCl}-\text{CsCl}$ and $\text{NaCl}-\text{CsCl}$ determined by Hersh and Kleppa,¹⁸ who found nearly ideal entropies of mixing in all three binaries. The enthalpy and entropy change for eqn. (9) can be calculated from data in Ref. 19: $\Delta_r H^\circ(900 \text{ K})[\text{eqn. (9)}] = 251 \text{ kJ mol}^{-1}$ and $\Delta_r S^\circ(900 \text{ K})[\text{eqn. (9)}] = 125 \text{ J K}^{-1} \text{ mol}^{-1}$.

Using these values and the partial enthalpy and entropy of mixing of AgCl calculated from the data of Hersh and Kleppa,¹⁸ together with eqn. (14) and the values of A and B , we obtain $\Delta_{\text{fus}} S_{\text{NbCl}_3} = 52 \text{ J K}^{-1} \text{ mol}^{-1}$ and $\Delta_{\text{fus}} H_{\text{NbCl}_3} + \Delta \bar{H}_{\text{NbCl}_3} = 37 \text{ kJ mol}^{-1}$. At low NbCl_3 concentrations ($x_{\text{NbCl}_3} < 0.002$), Henry's law is valid, and $\Delta \bar{H}_{\text{NbCl}_3}$ and γ_{NbCl_3} are constants. It is known from the literature that NbCl_3 does not melt below 900 K.¹⁶ Using the relation $\Delta_{\text{fus}} S T_{\text{fus}} = \Delta_{\text{fus}} H$, we can estimate that $\Delta_{\text{fus}} H > 47 \text{ kJ mol}^{-1}$. The partial enthalpy of mixing of NbCl_3 in a dilute solution of the $\text{NaCl}-\text{CsCl}_{\text{eutectic}}$ must then be less than -10 kJ mol^{-1} . Both YCl_3 and LaCl_3 show negative deviation from ideality^{20,21} in alkali chloride melts, and yttrium(III) and lanthanum(III) form octahedral complexes in chloride melts. The hypothetical

Table 3. Enthalpy, entropy and temperatures of fusion for selected MCl_3 salts.

Salt	$\Delta_{\text{fus}} H/\text{kJ mol}^{-1}$	$\Delta_{\text{fus}} S/\text{J K}^{-1} \text{ mol}^{-1}$	T_{fus}/K
NbCl_3	> 47	52	> 900
YCl_3	31.5	31.6	994
LaCl_3	54.4	48.1	1131
NdCl_3	50.2	48.7	1033
ScCl_3	67.4	54.3	1240

Table 4. Composition of the precipitated black solid on the Nb–electrode obtained from melts with $x_{\text{NbCl}_3} > 0.002$. The elemental analysis represents average values from 14 locations on the precipitated crystals.

Element	Atom (% \pm SD)
Na	4.04 \pm 1.18
Cs	18.56 \pm 1.08
Nb	12.19 \pm 0.38
Cl	65.21 \pm 0.78

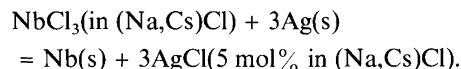
fusion data for NbCl₃ and fusion data for other higher melting metal trihalides are given in Table 3. When compared to these data, both the entropy and enthalpy of fusion of NbCl₃ seem reasonable.

To compare cell potentials from this work with the cell potentials by Picard and Bocage³ and Lantelme *et al.*⁴ in the LiCl–KCl eutectic melt at 450°C, it is necessary to correct for different standard states and different reference electrodes. Both Lantelme *et al.* and Picard and Bocage refer their potentials to the standard chlorine electrode. Lantelme *et al.* used a 1 molar NbCl₃ solution as standard state for NbCl₃, while Picard and Bocage used a 1 molal NbCl₃ solution. Inserting into eqn. (14) the mole fractions of NbCl₃ corresponding to one molar and one molal NbCl₃ solution in the LiCl–KCl eutectic, respectively, and correcting for the difference in potential between the chlorine electrode and the Ag/AgCl electrode used in this work, the potentials in the CsCl–NaCl supercooled eutectic at 450°C are –1.52 and –1.53 V, compared to –1.44 V³ and –1.48 V,⁴ respectively. The differences in the potentials are probably due to the higher stability of NbCl₃ in the NaCl–CsCl eutectic.

The black deposit formed on the Nb electrode when log $x_{\text{NbCl}_3} > -2.7$. The deposited crystals on the Nb electrode were removed after the experiment and analysed by a scanning electron microscope (Zeiss DSM 940) equipped with an X-ray analyser (Noran Instruments). The precipitate looked homogeneous when inspected visually and by SEM. Peaks belonging to Na, Cs, Nb and Cl were found in the X-ray spectrum. The crystals were broken, and a quantitative analysis of the contents of Na, Cs, Nb and Cl at 14 different locations is given in Table 4. Since we have Na⁺, Cs⁺ and Cl[–] in the deposit, the average valence state of niobium is calculated to be +3.5. Nb(III) therefore probably undergoes a disproportionation reaction that has a significant reaction rate at a concentration level of $x_{\text{NbCl}_3} > 0.002$. This concentration level seems to be independent of temperature in the range 600–700°C.

Conclusions

At mole fractions of NbCl₃ lower than 0.002 and in the temperature range 600–700°C, NbCl₃ seems to be in equilibrium with niobium metal, and the reversible cell reaction that takes place in the present galvanic cell is:



The partial enthalpy of mixing of NbCl₃ in the NaCl–CsCl eutectic melt using liquid NbCl₃ as standard state is calculated to be less than –10 kJ mol^{–1}. For $x_{\text{NbCl}_3} > 0.002$ in the NaCl–CsCl eutectic the reversible cell reaction is changed, and a precipitate is formed on the niobium electrode. The precipitate consists of niobium, sodium, caesium and chloride, with an average valence state of niobium equal to +3.5.

Acknowledgements. This project has benefitted scientifically from our participation in a Human Capital and Mobility Network. We appreciate interesting discussions with Prof. W. Freyland, University of Karlsruhe, Germany, and Prof. G.N. Papatheodorou, University of Patras, Greece, on the structure of niobium chloride containing melts. Financial support from the Norwegian Research Council is also gratefully acknowledged.

References

- Mellors, G. W. and Senderoff, S. J. *Electrochem. Soc.* 112 (1965) 266.
- Elizarova, I. R., Polyakov, E. G. and Polyakova, L. P. *Elektrokhimiya* 27 (1991) 640.
- Picard, G. and Bocage, P. *Mater. Sci. Forum.* 73–75 (1991) 505.
- Lantelme, F., Barhoun, A. and Chevalet, F. *J. Electrochem. Soc.* 140 (1993) 324.
- Kuznetsov, S. A., Morachevskii, A. G. and Stangrit, P. T. *Sov. Electrochem.* 18 (1982) 1357.
- Huber, K. and Jost, E. *Helv. Chim. Acta* 41 (1958) 2411.
- Dartnell, J., Johnson, K. E. and Shreir, L. L. *J. Less Common. Met.* 6 (1964) 85.
- Ivanovskii, L. E. and Krasil'nikov, M. T. *Electrochemistry of Molten Salts and Solid Electrolytes* 4 (1967) 71.
- Nakagava, I. and Hirabayashi, Y. *Denki Kagaku* 51 (1983) 256.
- Saeki, Y., Otani, M. and Suzuki, T. *J. Electrochem. Soc. Jpn.* 35 (1967) 42.
- Vasin, B. D., Maslov, S. V., Raspopin, S. P., Kalinin, M. G. and Sukhinin, D. B. *Raspilvy* 4 (1990) 48.
- Yang, L., Hudson, R. L. and Chien, C. Y. *Met. Soc. Conf.* 8 (1961) 925.
- Suzuki, T. *Electrochim. Acta* 15 (1970) 127.
- Rosenkilde, C. and Østvold, T. *Molten Salt Forum* 1–2 (1993–94) 87.
- Bachtler, M., Rockenberger, J., Freyland, W., Rosenkilde, C. and Østvold, T. *J. Phys. Chem.* 98 (1994) 742.
- Schäfer, H. and Dohmann, K.-D. *Z. Anorg. Allg. Chem.* 300 (1959) 1.
- Stern, K. H. *J. Electrochem. Soc.* 127 (1980) 2375.
- Hersh, L. S. and Kleppa, O. J. *J. Chem. Phys.* 42 (1965) 1309.
- Barin, I. *Thermochemical Data of Pure Substances*, VCH, Mannheim 1989.
- Papatheodorou, G. N. and Østvold, T. *J. Phys. Chem.* 78 (1974) 181.
- Papatheodorou, G. N., Wærnes, O. and Østvold, T. *Acta Chem. Scand., Ser. A* 33 (1979) 173.

Received February 23, 1994.